JACS
JOURNAL OF THE AMERICAN CHEMICAL SOCIETY
Article
pubs.acs.org/JACS

New-Structure-Type Fe-Based Superconductors: $CaAFe_4As_4$ (A = K, Rb, Cs) and $SrAFe_4As_4$ (A = Rb, Cs)

Akira Iyo,*[,†] Kenji Kawashima,[†,‡] Tatsuya Kinjo,[†,§] Taichiro Nishio,[†,§] Shigeyuki Ishida,[†] Hiroshi Fujihisa,[†] Yoshito Gotoh,[†] Kunihiro Kihou,[†] Hiroshi Eisaki,[†] and Yoshiyuki Yoshida[†]

[†]National Institute of Advanced Industrial Science and Technology (AIST), 1-1-1 Umezono, Tsukuba, Ibaraki 305-8568, Japan
[‡]IMRA Material R&D Co., Ltd., 2-1 Asahi-machi, Kariya, Aichi 448-0032, Japan
[§]Department of Physics, Tokyo University of Science, 1-3 Kagurazaka, Shinjuku, Tokyo 162-8601, Japan

Supporting Information

ABSTRACT: Fe-based superconductors have attracted research interest because of their rich structural variety, which is due to their layered crystal structures. Here we report the new-structure-type Fe-based superconductors $CaAFe_4As_4$ (A = K, Rb, Cs) and $SrAFe_4As_4$ (A = Rb, Cs), which can be regarded as hybrid phases between $AeFe_2As_2$ (Ae = Ca, Sr) and AFe_2As_2. Unlike solid solutions such as $(Ba_{1-x}K_x)Fe_2As_2$ and $(Sr_{1-x}Na_x)Fe_2As_2$, Ae and A do not occupy crystallographically equivalent sites because of the large differences between their ionic radii. Rather, the Ae and A layers are inserted alternately between the Fe_2As_2 layers in the c-axis direction in $AeAFe_4As_4$ ($AeA1144$). The ordering of the Ae and A layers causes a change in the space group from $I4/mmm$ to $P4/mmm$, which is clearly apparent in powder X-ray diffraction patterns. $AeA1144$ is the first known structure of this type among not only Fe-based superconductors but also other materials. $AeA1144$ is formed as a line compound, and therefore, each $AeA1144$ has its own superconducting transition temperature of approximately 31−36 K.

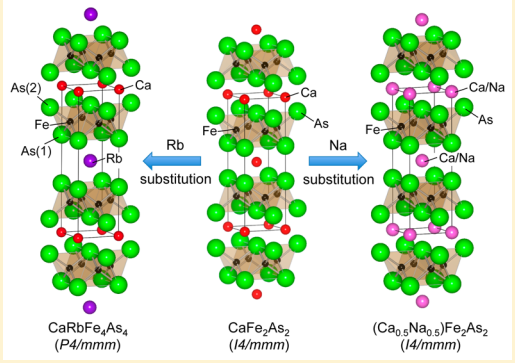

INTRODUCTION

The Fe-based superconductors discovered in 2008 by Kamihara et al.[1] have attracted significant research interest because of their rich material variety as well as their high superconducting transition temperatures (T_c).[2] The material variations are due to the layered crystal structures of these superconductors. A large number of related Fe-based superconductors with various types of crystal structures have been found to date.[3] The search for materials with new structural types is important because it can trigger further discovery of new superconductors. In fact, such discoveries often occur in relation to both Fe-based and Cu-based superconductors.

Superconductors based on $AeFe_2As_2$ (Ae = Ca, Sr, Ba (alkaline-earth metal)) parent compounds with a $ThCr_2Si_2$-type structure ($I4/mmm$), i.e., the so-called "122" system, are the most popular materials for both physical explorations and wire applications because of their high upper critical fields and low anisotropies.[4] Superconductivity in $AeFe_2As_2$ is primarily induced by alkali metal (A = Na, K, Rb, Cs) substitution at Ae sites. The structure's crystallographic space group ($I4/mmm$) is not changed by this A substitution because Ae and A randomly occupy crystallographically equivalent sites. Thus, $(Ae_{1-x}A_x)Fe_2As_2$ ($(Ae,A)Fe_2As_2$) are solid solutions between $AeFe_2As_2$ and AFe_2As_2 compounds with the same structural type.

$(Ba,K)Fe_2As_2$ is the first high-T_c superconductor induced in $AeFe_2As_2$.[5] The T_c of this material varies depending on the substituted K fraction, and the maximum T_c can be as high as 38 K. Triggered by the discovery of $(Ba,K)Fe_2As_2$, superconductors with similar structural types have been found for several combinations of Ae and A: $(Ca,Na)Fe_2As_2$,[6−8] $(Ca,K)Fe_2As_2$,[9] $(Sr,Na)Fe_2As_2$,[10,11] $(Sr,K)Fe_2As_2$,[12] $(Sr,Cs)Fe_2As_2$,[12] $(Ba,Na)Fe_2As_2$,[13] and $(Ba,Rb)Fe_2As_2$.[14] However, superconductor materials formed by combinations of Ae and A with large differences between their ionic radii (Δr), such as Ca and Rb or Ca and Cs, have not yet been realized.

In this paper, we report Fe-based superconductors with a new structural type, $CaAFe_4As_4$ (A = K, Rb, Cs) and $SrAFe_4As_4$ (A = Rb, Cs), hereafter abbreviated as $AeA1144$. These materials include the above-mentioned unrealized Ae and A combinations. Because A does not mix with Ae in such cases as a result of the large Δr, $AeA1144$ crystallizes through alternate stacking of the Ae and A layers across the Fe_2As_2 layer. The ordering of the Ae and A layers changes the space group from $I4/mmm$ to $P/4\ mmm$. $AeA1144$ is formed as a line compound, and all of the $AeA1144$ compounds are found to have superconductivity at their own T_c values of approximately 31−36 K.

Received: December 2, 2015
Published: March 4, 2016

DOI: 10.1021/jacs.5b12571
J. Am. Chem. Soc. 2016, 138, 3410−3415

EXPERIMENTAL PROCEDURE

Polycrystalline *Ae*A1144 samples were synthesized using the stainless steel (SUS) pipe and cap method, which has been described elsewhere.[11] The *Ae*As, *A*As, FeAs, and Fe_2As starting materials were prepared via the reaction of *Ae*, *A*, or Fe with As. The starting materials were ground with an agate mortar in a nitrogen-filled glovebox and pressed into a pellet. Excess *Ae*, *A*, and As were employed in the starting compositions at 10−15 atom %, taking into account element evaporation during heating in the pipe. A pellet weighing approximately 0.2 g was placed directly into an SUS pipe with outer and inner diameters of 8 and 6 mm, respectively, and a length of 60 mm. Both ends of the pipe were sealed with tube-fitting caps.

The SUS pipe was placed inside a preheated furnace in order to suppress the formation of stable *Ae*122 and *A*122 at lower temperatures (*T*). The sample was heated to 860−920 °C, depending on the specific *A* and *Ae* combination, for 2−6 h; this was followed by rapid cooling to room temperature (RT). It should be noted that the part of the sample in contact with the pipe was degraded through reaction with the pipe; this degraded part was removed mechanically. The reaction process was repeated following intermediate pulverization and the addition of 15−20 atom % As. Samples of $(Ca_{0.5}Na_{0.5})Fe_2As_2$ ($(Ca_{0.5}Na_{0.5})122$) and $(Sr_{0.5}K_{0.5})Fe_2As_2$ ($(Sr_{0.5}K_{0.5})122$) were synthesized using a similar method for the purpose of comparison.

Powder X-ray diffraction (XRD) patterns were measured at RT using a diffractometer with Cu Kα radiation (Rigaku, Ultima IV) equipped with a high-speed detector system (Rigaku, D/teX Ultra). The lattice constants and the atomic positions were refined via Rietveld analysis using the software Materials Studio Reflex.[16] Magnetization (*M*) measurements were performed under a magnetic field (*H*) of 10 Oe using a magnetic property measurement system (Quantum Design MPMS-XL7). The electrical resistivity was measured using a four-probe method.

RESULTS

Powder XRD Analysis. Figure 1 shows the XRD pattern obtained for CaRb1144 as a representative of *Ae*A1144, together with that of $(Ca_{0.5}Na_{0.5})122$ for comparison. The diffraction indices of the $(Ca_{0.5}Na_{0.5})122$ *hkl* peaks are assigned on the basis of a body-centered tetragonal structure with space group *I*4/*mmm* ($ThCr_2Si_2$-type structure), for which only even values of $h + k + l$ can appear in accordance with the *I*4/*mmm* extinction rule, as indexed in Figure 1.

On the other hand, we note that additional peaks that cannot be assigned to the $ThCr_2Si_2$-type structure are apparent in the case of CaRb1144, as indicated by the arrows in Figure 1. These additional peaks can be indexed by assuming a primitive tetragonal structure with space group *P*4/*mmm*. Because no extinction rule applies to *P*4/*mmm*, peaks with *hkl* diffraction indices corresponding to odd values of $h + k + l$ can appear. The presence of such extra peaks shows that the CaRb1144 crystal structure differs fundamentally from that of $(Ca_{0.5}Na_{0.5})$-122.

The change in the space group can be explained by assuming that the Ca and Rb layers stack alternately across the Fe_2As_2 layer in CaRb1144 whereas Ca and Na are randomly mixed in the (Ca,Na) layers in $(Ca_{0.5}Na_{0.5})122$, as shown in Figure 1. The ordering of the Ca and Rb layers changes the space group from body-centered tetragonal *I*4/*mmm* to primitive tetragonal *P*4/*mmm*. This assumption is supported by the crystal structure refinement analysis, as shown below.

Similar characteristic diffraction patterns were also observed for Ca*A*1144 (*A* = K, Cs) and Sr*A*1144 (*A* = Rb, Cs) samples (see Figure S1 in the Supporting Information), which strongly indicates that the samples have the same crystal structure type as CaRb1144. The lattice parameters of *Ae*A1144 obtained through least-squares fitting of the *d* values of the peaks are listed in Table I, together with those of *Ae*122 and *A*122. The *a* and *c* lattice parameters of Ca*A*1144 (Sr*A*1144) are located almost centrally with respect to those of Ca122 (Sr122) and *A*122, which is both reasonable and consistent with the above structural picture.

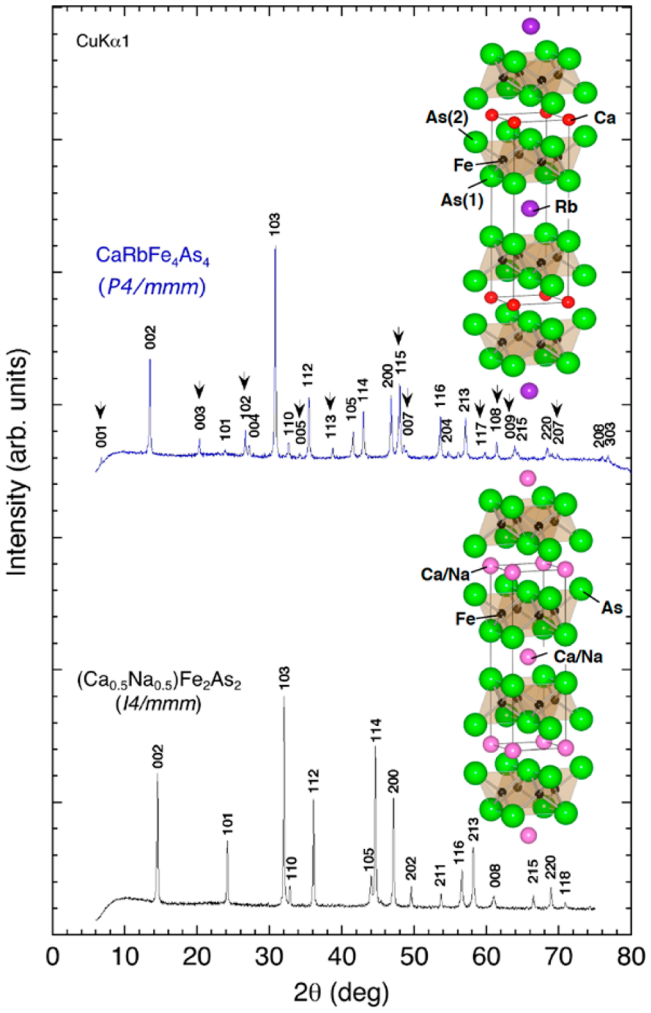

Figure 1. Powder XRD pattern of $CaRbFe_4As_4$, together with that of $(Ca_{0.5}Na_{0.5})Fe_2As_2$ for comparison. All of the peaks are identified as corresponding to a $ThCr_2Si_2$-type structure for $(Ca_{0.5}Na_{0.5})Fe_2As_2$. The $CaRbFe_4As_4$ peaks are indexed on the basis of a primitive tetragonal structure with space group *P*4/*mmm*. Peaks that can appear for *P*4/*mmm* only are indicated by arrows. The crystal structures are depicted using VESTA.[21] The solid lines represent unit cells.

Crystal Structure Refinement. We performed crystal structure refinement for CaRb1144, and Figure 2 shows the powder XRD pattern and Rietveld refinement for this material. The crystal structure model expected from the XRD analysis fits the diffraction pattern with a weighted-profile reliability factor (R_{wp}) of 11.0% and an expected reliability factor (R_e) of 7.7%. These values are sufficiently small to allow us to conclude that the assumed crystal structural model is appropriate.

The refined structural parameters of CaRb1144 are summarized in Table II. Furthermore, the CaRb1144 crystal structure is illustrated in the inset of Figure 1 using the obtained structure parameters, together with that of $(Ca_{0.5}Na_{0.5})122$ for comparison.[20] Ca and Rb in CaRb1144 occupy separate unique sites, whereas Ca and Na in

DOI: 10.1021/jacs.5b12571
J. Am. Chem. Soc. 2016, 138, 3410−3415

Table I. Space Groups, Lattice Parameters, and T_c Values for $AeAFe_4As_4$, $AeFe_2As_2$, and AFe_2As_2

compound	space group[a]	a (Å)	c (Å)	T_c (K)	ref
$CaKFe_4As_4$	P	3.866(1)	12.817(5)	33.1	this work[b]
$CaRbFe_4As_4$	P	3.8757(9)	13.104(3)	35.0	this work[b]
$CaCsFe_4As_4$	P	3.891 (1)	13.414(2)	31.6	this work[b]
$SrRbFe_4As_4$	P	3.897(1)	13.417(5)	35.1	this work[b]
$SrCsFe_4As_4$	P	3.910(1)	13.729(3)	36.8	this work[b]
$BaCsFe_4As_4$ or $(Ba,Cs)Fe_2As_2$	P or I	3.927(2)	14.134(6)	26	this work[b]
$CaFe_2As_2$	I	3.900(1)	11.62(1)	NS[c]	6
$SrFe_2As_2$	I	3.9266(5)	12.370(2)	NS[c]	11
$BaFe_2As_2$	I	3.9612(3)	13.006(1)	NS[c]	15
$NaFe_2As_2$	I	3.8090(5)	12.441(3)	25	17
KFe_2As_2	I	3.8414(2)	13.837(1)	3.8	12
$RbFe_2As_2$	I	3.888(2)	14.534(7)	2.6	18, 19
$CsFe_2As_2$	I	3.8894(2)	15.066(5)	1.8	12

[a] $P = P4/mmm$; $I = I4/mmm$. [b] T_c was determined from the onset temperature of the superconducting transition measured via magnetization. [c] NS = nonsuperconductor at ambient pressure.

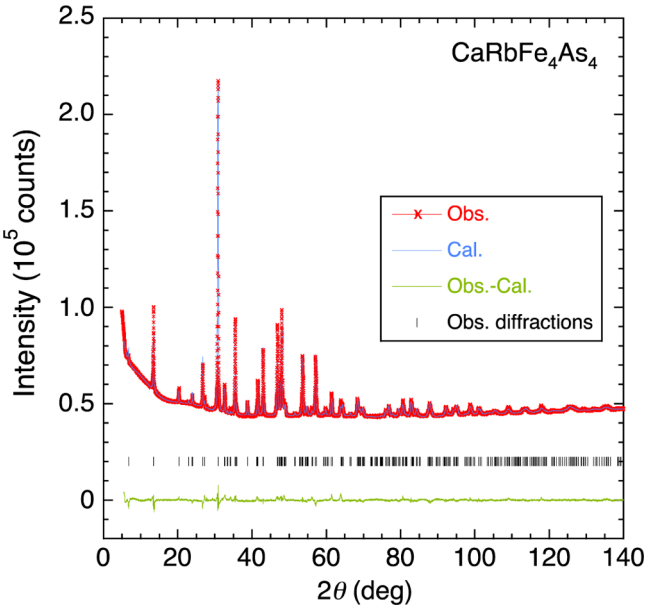

Figure 2. Powder XRD pattern and Rietveld refinement of $CaRbFe_4As_4$ (Obs. = observed; Cal. = calculated).

Table II. Atomic Coordinates and Isotropic Displacement Parameters (U_{iso}) of $CaRbFe_4As_4$ at RT[a]

atom	x	y	z	$1000U_{iso}$ (Å^2)
Ca	0	0	0	6.6(8)
Rb	0.5	0.5	0.5	9.8(4)
Fe	0	0.5	0.2246(1)	7.7(3)
As(1)	0	0	0.3336(1)	6.9(3)
As(2)	0.5	0.5	0.1193(1)	6.9(3)

[a] Space group: $P4/mmm$. a = 3.8778(1) Å, c = 13.1088(1) Å. V = 197.12(1) Å^3. Z = 1. R_{wp} = 11.0%, R_e = 7.7%, S = 1.42. Preferred orientation parameter (R_0) = 1.838(4), direction = ⟨0.501, 0.198, 0.842⟩. The occupancy is fixed to 1 at all atomic sites. Selected structural parameters: $d_{Fe-As(1)}$ = 2.408(2) Å; $d_{Fe-As(2)}$ = 2.380(2) Å; $h_{As(1)}$ = 1.429(3) Å; $\alpha_{As(1)-Fe-As(1)}$ = 107.2(1)°; $\alpha_{As(2)-Fe-As(2)}$ = 109.1(1)°; $h_{As(1)}$ = 1.429(3) Å; $h_{As(2)}$ = 1.381(3) Å.

$(Ca_{0.5}Na_{0.5})122$ are mixed on the same sites. CaRb1144 can be regarded as a hybrid phase between Ca122 and Rb122. The variation in crystal structure is considered to be based on the ionic radii of Rb and Na. That is, the Δr between Ca^{2+} and Rb^+ (0.49 Å) is too large for these components to mix with each other, whereas the ionic radius of Na^+ is almost identical to that of Ca^{2+} (the difference is only 0.06 Å).[22]

We wish to briefly mention the single-crystal growth of $AAe1144$. We attempted to grow CaRb1144 and CaK1144 single crystals using RbAs and KAs fluxes,[23] respectively, for more precise structural analysis. However, only Rb122 and K122 crystals were obtained. Appropriate fluxes and/or growth methods must be determined in order to obtain single crystals.

Superconducting Transition Temperatures. Figure 3a,b shows the T dependence of the magnetization divided by the applied field, M/H, for CaA1144 (A = K, Rb, Cs) and SrA1144 (A = Rb, Cs), respectively. All of the samples exhibit superconducting transitions that are sufficiently sharp to allow the onset T_c to be clearly defined. The zero-field-cooled (ZFC) magnetizations at 5 K are sufficiently large as bulk superconductors ($4\pi M/H = -1$ corresponds to perfect diamagnetism). The onset T_c for each sample is listed in Table I. The AeA1144 samples have T_c values within the 30 K region, similar to $(Ae,A)122$ compounds. SrCs1144 has the highest T_c of 36.8 K, which is comparable to those of $(Sr_{0.6}K_{0.4})Fe_2As_2$ (T_c = 37 K)[12] and $(Ba_{0.6}K_{0.4})Fe_2As_2$ (T_c = 38 K).[5]

Figure 4a,b shows the T dependence of the resistivity $\rho(T)$ for CaA1144 (A = K, Rb, Cs) and SrAFe_4As_4 (A = Rb, Cs), respectively. The CaA1144 exhibit onset T_c values of 33.4, 34.6, and 32.0 K for A = K, Rb, and Cs, respectively. The SrA1144 have onset T_c values of 35.7 and 37.0 K for A = Rb and Cs, respectively. These values of T_c are close to those determined from the magnetization measurements. The normal-state $\rho(T)$ exhibits metallic behavior with convex curvature, which resembles the behavior observed for $(Ae,A)122$ samples.[5,6]

Line-Phase Nature of $AAe1144$. Because $AAe1144$ is crystallized through ordering of the A and Ae layers, the compound is formed as a line phase, i.e., the atomic ratio of elements in the crystal is fixed. In order to demonstrate this characteristic feature directly, we synthesized a sample with a nominal composition of $Ca_{1.5}K_{0.5}Fe_4As_4$. The sample separated into two phases in accordance with the formula $Ca_{1.5}K_{0.5}Fe_4As_4 \rightarrow 0.5CaKFe_4As_4 + CaFe_2As_2$ (see Figure S2 in the Supporting Information). The a- and c-axis lattice parameters and the T_c of the CaK1144 phase in the sample are 3.869(3) Å, 12.804(5) Å, and 33.9 K, respectively, which are close to the results for the CaK1144 sample given in Table I. This behavior never occurs

DOI: 10.1021/jacs.5b12571
J. Am. Chem. Soc. 2016, 138, 3410−3415

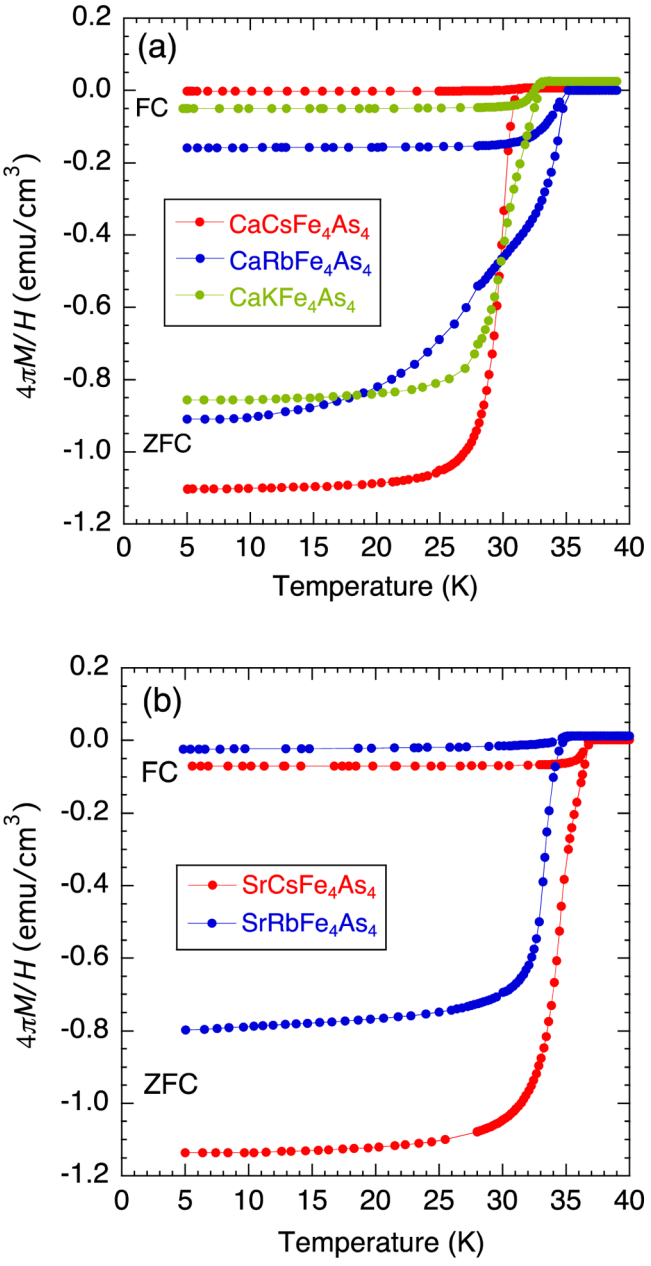

Figure 3. Temperature dependence of the magnetization divided by the applied field, M/H, for (a) CaAFe$_4$As$_4$ (A = K, Rb, Cs) and (b) SrAFe$_4$As$_4$ (A = Rb, Cs). The magnetization was measured using zero-field-cooled (ZFC) and field-cooled (FC) processes.

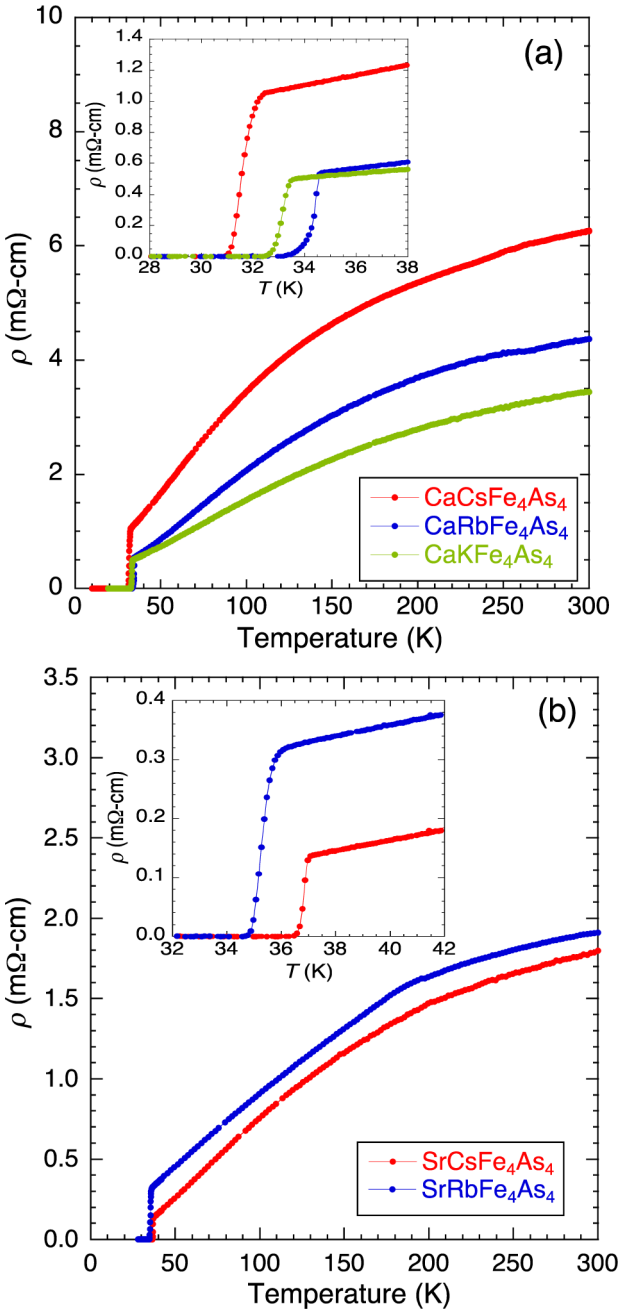

Figure 4. Temperature dependence of the resistivity $\rho(T)$ for (a) CaAFe$_4$As$_4$ (A = K, Rb, Cs) and (b) SrAFe$_4$As$_4$ (A = Rb, Cs). The insets exhibit enlargements near the superconducting transitions at low temperature.

for (Ae,A)122 solid solutions. Therefore, this experiment clearly demonstrates the line-phase nature of AAe1144.

Synthesis of the BaCsFe$_4$As$_4$ Phase. We attempted to synthesize BaCsFe$_4$As$_4$ samples by varying the synthesis conditions over a wide range. However, we were unable to obtain sufficiently high quality samples to determine the structural type (see Figure S3 in the Supporting Information). The sample exhibits superconductivity at 26 K. The lattice parameters of (Ba,Cs)122 or BaCs1144 are estimated to be a = 3.927(2) Å and c = 14.134(6) Å. The lattice parameters are almost centrally positioned relative to those of Ba122 and Cs122, which may indicate that the sample has a line-phase nature. However, extra peaks that would appear only for the $P4/mmm$ space group are not apparent in the diffraction pattern. Furthermore, the peak broadening and low peak intensity prevented us from determining the structural type. Improved sample quality is necessary to yield a conclusive result.

DISCUSSION

***AAe*1144 Crystal Structure.** To the best of our knowledge, this is the first time the crystal structure type determined via the Rietveld analysis of CaRb1144 has been reported, not only for Fe-based superconductors but also for other materials. Although we have not refined the crystal structures of the other CaAFe$_4$As$_4$ (A = K, Cs) and SrAFe$_4$As$_4$ (A = Rb, Cs) samples, their distinctive diffraction patterns provide sufficiently

DOI: 10.1021/jacs.5b12571
J. Am. Chem. Soc. 2016, 138, 3410−3415

strong evidence to allow us to conclude that all of these samples have the same structure type as CaRb1144.

In CaRb1144, the Fe layer is located in closer proximity to the Ca layer than the Rb layer, as indicated by the atomic coordinate of Fe (z = 0.225) in Table II. The displacement of the Fe layer can be naturally understood by considering the valences of the constituting layers. The negatively charged Fe_2As_2 layer ($(Fe_2As_2)^{1.5-}$) is more strongly attracted by the Ca^{2+} layer than by the Rb^+ layer. This is in contrast to $(Ca_{0.5}Na_{0.5})122$, in which the Fe_2As_2 layers are exactly centrally positioned between the $(Ca_{0.5}Na_{0.5})$ layers.

Furthermore, the As around Fe are no longer crystallographically equivalent. The Fe−As interatomic distance is divided into two different values: $d_{Fe-As(1)}$ = 2.408(2) Å and $d_{Fe-As(2)}$ = 2.380(2) Å for the Rb- and Ca-layer sides, respectively. Consequently, two different As−Fe−As bond angles ($\alpha_{As-Fe-As}$) and As heights from the Fe layers (h_{As}) exist in CaRb1144. These are empirically important parameters governing T_c in Fe-based superconductors.[24,25] The As−Fe−As bond angle for the Ca-layer side ($\alpha_{As(1)-Fe-As(1)}$ = 109.1°) is close to that of a regular tetrahedron (109.5°), while that for the Rb layer side ($\alpha_{As(2)-Fe-As(2)}$ = 107.2°) is smaller than $\alpha_{As(1)-Fe-As(1)}$. Although the effect of the unequal As−Fe−As bond angles on T_c seems to be small, as the 1144- and 122-type superconductors exhibit similar T_c values, the electronic structure of *AAe*1144 is an interesting topic for future study.

Line-Phase Nature of *AAe*1144. It is well-known that the T_c values of $(Ae_{1-x}A_x)122$ systems vary depending on the composition (x) value (formal Fe valence). In $AeAFe_4As_4$, the Fe valence state is fixed at 2.25+, which is centrally positioned between the values of 2.0+ and 2.5+ for *Ae*122 and *A*122, respectively. Therefore, each *AeA*1144 compound must have its own T_c and lattice parameters in principle (small deviations can occur as a result of lattice defects). This is the origin of the robustness of T_c against composition deviation in the 1144 line phase, as confirmed above.

We determined that the $SrCsFe_4As_4$ and $CaKFe_4As_4$ samples belong to *AeA*1144 on the basis of their characteristic XRD patterns. On the other hand, superconductivity at 37 K has been reported for $(Sr_{0.6}Cs_{0.4})Fe_2As_2$ by Sasmal et al.[12] Those researchers reported that $(Sr_{1-x}Cs_x)Fe_2As_2$ has a phase diagram (which was not shown in their paper) similar to that of the $(Sr_{1-x}K_x)Fe_2As_2$ system. They synthesized $(Sr_{1-x}Cs_x)Fe_2As_2$ samples from mixtures of $SrFe_2As_2$ and $CsFe_2As_2$ in welded Nb containers. Wang et al.[9] reported superconductivity at 35.5 K for a $(Ca_{0.6}K_{0.4})Fe_2As_2$ single crystal grown via an FeAs flux method. The experimental data concerning the crystal structures were not supplied for the $(Sr_{0.6}Cs_{0.4})Fe_2As_2$ and $(Ca_{0.6}K_{0.4})Fe_2As_2$ samples. It may be possible to obtain solid-solution $(Sr,Cs)Fe_2As_2$ and $(Ca,K)Fe_2As_2$ depending on the synthesis process.

Conditions for 1144 Phase Formation. As already mentioned, Δr is an important factor affecting the formation of the 1144 phase. In addition, we found that the difference between the a-axis lattice parameters of *Ae*122 and *A*122 is also meaningful in regard to the formation of the 1144 and 122 phases. The ionic radii (VIII coordination) of the *Ae* ions (r^{Ae}) are 1.42, 1.26, and 1.12 for Ba, Sr, and Ca, respectively, and those of the *A* ions (r^A) are 1.74, 1.61, 1.51, and 1.18 Å for Cs, Rb, K, and Na, respectively.[22] The a-axis lattice parameters of *Ae*122 (a^{Ae122}) and *A*122 (a^{A122}) are listed in Table I.

Figure 5 shows the relationship between Δr ($= r^A - r^{Ae}$) and Δa ($= a^{A122} - a^{Ae122}$) for the *Ae* and *A* combinations given in *AeA* form in Figure 5. The solid squares and circles show the *AeA* that yield the 1144 and 122 phases, respectively. The data are clearly separated into two phase regions, one for 1144 and the other for 122. Figure 5 suggests that a small Δa as well as a large Δr are necessary for the formation of the 1144 phases. BaCs, whose structural type is unknown, is located at the boundary between the 1144 and 122 phases; this may partly explain the sample synthesis difficulties. This kind of analysis can provide guidance for the exploration of new 1144 compounds in materials other than Fe-based superconductors.

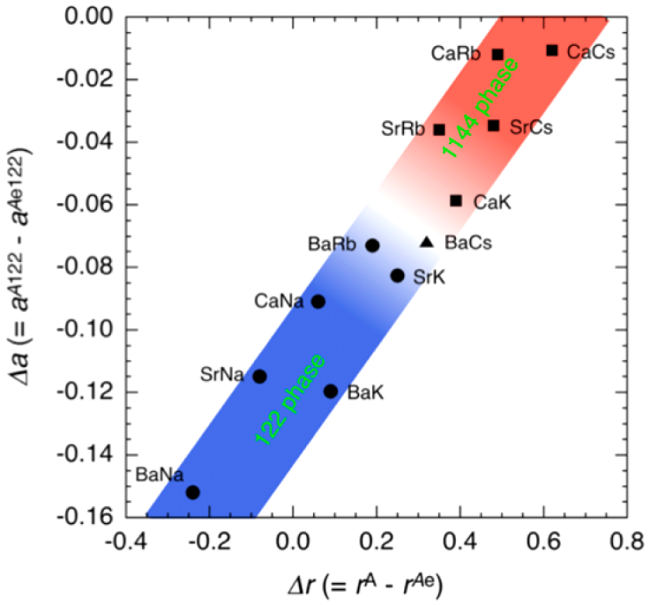

Figure 5. Plot of Δa vs Δr for the *Ae* and *A* combinations in $AeAFe_4As_4$. The solid squares and circles show the *AeA* that yield 1144 and 122 phases, respectively. BaCs, whose structural type has not yet been determined, is indicated by a solid triangle.

SUMMARY

We found Fe-based superconductors with a new structural type, *CaA*1144 (*A* = K, Rb, Cs) and *SrA*1144 (*A* = Rb, Cs), with T_c values of approximately 31−36 K. Because *AeA*1144 is formed as a line compound, each *AeA*1144 material has unique lattice parameters and T_c, unlike $(Ae_{1-x}A_x)Fe_2As_2$ solid solutions. Consequently, the T_c of *AeA*1144 is robust against deviations in the sample composition. This property may be beneficial in regard to applications of these materials. However, details of the superconducting properties, such as information on the critical fields, critical current densities, and anisotropy, remain unclear. Further experimental and theoretical investigations are desired. The discovery of *AeA*1144 appends a new structural type to the structure database as well as to Fe-based superconductors. Analysis of the conditions for phase formation may provide guidance in the search for new 1144-type compounds.

ASSOCIATED CONTENT

Supporting Information

The Supporting Information is available free of charge on the ACS Publications website at DOI: 10.1021/jacs.5b12571.

XRD patterns for $CaAFe_4As_4$ (*A* = K, Cs) and $SrAFe_4As_4$ (*A* = Rb, Cs) and XRD patterns and *T*-dependent

DOI: 10.1021/jacs.5b12571
J. Am. Chem. Soc. 2016, 138, 3410−3415

magnetizations of the samples with nominal compositions $Ca_{1.5}K_{0.5}Fe_4As_4$ and $BaCsFe_4As_4$ (PDF)

AUTHOR INFORMATION

Corresponding Author

*iyo-akira@aist.go.jp

Notes

The authors declare no competing financial interest.

ACKNOWLEDGMENTS

We are grateful to Dr. Hirofumi Kawanaka for support with the sample preparation. We thank Editage (www.editage.jp) for English language editing.

REFERENCES

(1) Kamihara, Y.; Watanabe, T.; Hirano, M.; Hosono, H. *J. Am. Chem. Soc.* **2008**, *130*, 3296−3297.
(2) Chen, X.; Dai, P.; Feng, D.; Xiang, T.; Zhang, F. C. *Natl. Sci. Rev.* **2014**, *1*, 371−395.
(3) Tanabe, K.; Hosono, H. *Jpn. J. Appl. Phys.* **2012**, *51*, 010005.
(4) Ma, Y. *Supercond. Sci. Technol.* **2012**, *25*, 113001.
(5) Rotter, M.; Tegel, M.; Johrendt, D.; Schellenberg, I.; Hermes, W.; Pöttgen, R. *Phys. Rev. B: Condens. Matter Mater. Phys.* **2008**, *78*, 020503.
(6) Shirage, P. M.; Miyazawa, K.; Kito, H.; Eisaki, H.; Iyo, A. *Appl. Phys. Express* **2008**, *1*, 081702.
(7) Wu, G.; Chen, H.; Wu, T.; Xie, Y. L.; Yan, Y. J.; Liu, R. H.; Wang, X. F.; Ying, J. J.; Chen, X. H. *J. Phys.: Condens. Matter* **2008**, *20*, 422201.
(8) Zhao, K.; Liu, Q. Q.; Wang, X. C.; Deng, Z.; Lv, Y. X.; Zhu, J. L.; Li, F. Y.; Jin, C. Q. *J. Phys.: Condens. Matter* **2010**, *22*, 222203.
(9) Wang, D. M.; Shangguan, X. C.; He, J. B.; Zhao, L. X.; Long, Y. J.; Wang, P. P.; Wang, L. *J. Supercond. Novel Magn.* **2013**, *26*, 2121−2124.
(10) Cortes-Gil, R.; Clarke, S. J. *Chem. Mater.* **2011**, *23*, 1009−1016.
(11) Shinohara, N.; Tokiwa, K.; Fujihisa, H.; Gotoh, Y.; Ishida, S.; Kihou, K.; Lee, C. H.; Eisaki, H.; Yoshida, Y.; Iyo, A. *Supercond. Sci. Technol.* **2015**, *28*, 062001.
(12) Sasmal, K.; Lv, B.; Lorenz, B.; Guloy, A. M.; Chen, F.; Xue, Y.-Y.; Chu, C.-W. *Phys. Rev. Lett.* **2008**, *101*, 107007.
(13) Avci, S.; Allred, J. M.; Chmaissem, O.; Chung, D. Y.; Rosenkranz, S.; Schlueter, J. A.; Claus, H. A.; Daoud-Aladine; Khalyavin, D. D.; Manuel, P.; Llobet, A.; Suchomel, M. R.; Kanatzidis, M. G.; Osborn, R. *Phys. Rev. B: Condens. Matter Mater. Phys.* **2013**, *88*, 094510.
(14) Bukowski, Z.; Weyeneth, S.; Puzniak, R.; Moll, P.; Katrych, S.; Zhigadlo, N. D.; Karpinski, J.; Keller, H.; Batlogg, B. *Phys. Rev. B: Condens. Matter Mater. Phys.* **2009**, *79*, 104521.
(15) Jiang, S.; Xing, H.; Xuan, G.; Wang, C.; Ren, Z.; Feng, C.; Dai, J.; Xu, Z.; Cao, G. *J. Phys.: Condens. Matter* **2009**, *21*, 382203.
(16) Dassault Systemes, BIOVIA Corporation. Materials Studio Reflex website. http://accelrys.com/products/collaborative-science/biovia-materials-studio/analytical-and-crystallization-software.html (accessed Jan 4, 2016).
(17) Gooch, M.; Lv, B.; Sasmal, K.; Tapp, J. H.; Tang, Z. J.; Guloy, A. M.; Lorenz, B.; Chu, C. W. *Phys. C* **2010**, *470*, S276−S279.
(18) Wenz, P.; Schuster, H. U. *Z. Naturforsch., B: J. Chem. Sci.* **1984**, *39*, 1816−1818.
(19) Bukowski, Z.; Weyeneth, S.; Puzniak, R.; Karpinski, J.; Batlogg, B. *Phys. C* **2010**, *470*, S328−S329.
(20) Zhao, K.; Liu, Q. Q.; Wang, X. C.; Deng, Z.; Lv, Y. X.; Zhu, J. L.; Li, F. Y.; Jin, C. Q. *Phys. Rev. B: Condens. Matter Mater. Phys.* **2011**, *84*, 184534.
(21) Momma, K.; Izumi, F. *J. Appl. Crystallogr.* **2008**, *41*, 653.
(22) Shannon, R. D. *Acta Crystallogr., Sect. A: Cryst. Phys., Diffr., Theor. Gen. Crystallogr.* **1976**, *32*, 751−767.
(23) Kihou, K.; Saito, T.; Ishida, S.; Nakajima, M.; Tomioka, Y.; Fukazawa, H.; Kohori, Y.; Ito, T.; Uchida, S.; Iyo, A.; Lee, C.-H.; Eisaki, H. *J. Phys. Soc. Jpn.* **2010**, *79*, 124713.
(24) Lee, C.-H.; Iyo, A.; Eisaki, H.; Kito, H.; Fernandez-Diaz, M. T.; Ito, T.; Kihou, K.; Matsuhata, H.; Braden, M.; Yamada, K. *J. Phys. Soc. Jpn.* **2008**, *77*, 083704.
(25) Mizuguchi, Y.; Hara, Y.; Deguchi, K.; Tsuda, S.; Yamaguchi, T.; Takeda, K.; Kotegawa, H.; Tou, H.; Takano, Y. *Supercond. Sci. Technol.* **2010**, *23*, 054013.

DOI: 10.1021/jacs.5b12571
J. Am. Chem. Soc. 2016, 138, 3410−3415